Catalysis Communications 52 (2014) 72–77

Contents lists available at ScienceDirect

Catalysis Communications

journal homepage: www.elsevier.com/locate/catcom

Short Communication

Determining *in situ* phases of a nanoparticle catalyst *via* grand canonical Monte Carlo simulations with the ReaxFF potential

Thomas P. Senftle [a], Adri C.T. van Duin [b,*], Michael J. Janik [a,*]

[a] Department of Chemical Engineering, Pennsylvania State University, University Park, PA 16802, USA
[b] Department of Mechanical and Nuclear Engineering, Pennsylvania State University, University Park, PA 16802, USA

ARTICLE INFO

Article history:
Received 5 September 2013
Received in revised form 28 November 2013
Accepted 2 December 2013
Available online 10 December 2013

Keywords:
Nanoparticle
Palladium
GC-MC
Oxidation
Carbide formation

ABSTRACT

Catalyst design requires a detailed understanding of the structure of the catalyst surface as a function of varying reaction conditions. Here we demonstrate the capability of a grand canonical Monte Carlo/molecular dynamics (GC-MC/MD) method utilizing the ReaxFF potential to predict nanoparticle structure and phase stability as a function of temperature and pressure. This is demonstrated for Pd nanoparticles, which readily form oxide, hydride, and carbide phases under reaction environments, impacting catalytic behavior. The approach presented here can be extended to other catalytic systems, providing a new tool for exploring the effects of reaction conditions on catalyst activity, selectivity, and stability.

1. Introduction

The rational design of catalytic systems featuring nano-sized metal particles requires knowledge of the active surface phase under operating conditions [1]. In particular, the reactant gas phase can rearrange the metal lattice, forming unique surface, subsurface, and bulk phases [1,2]. The chemical properties of such phases will differ from those of the parent metal, affecting the selectivity and activity of the catalyst [1–7]. Quantum mechanical (QM) computational methods, such as density functional theory (DFT), can model the phase stability of the catalyst through the formalism of *ab initio* thermodynamics [6,8–12]. The computational expense of QM methods, however, limits QM studies to highly idealized catalyst models. This has motivated the use of empirical force fields, such as ReaxFF [13], that are computationally inexpensive compared to QM, therefore helping to close the size and pressure gap between macroscopic experimental techniques and quantum-scale computational methods.

Herein, we demonstrate how the ReaxFF potential can be employed in hybrid grand canonical Monte Carlo/molecular dynamics (GC-MC/MD) simulations to determine the structure and stability of nanoparticle phases as a function of temperature and gas phase composition under reaction conditions. Phase reconstruction under operating conditions is a particular concern for Pd-based systems, which are industrially relevant oxidation [14–16] and hydrogenation catalysts [5–7]. Pd catalysts form oxide phases when employed under oxidizing conditions [3,4,17], and form complex hydride/carbide phases when used to hydrogenate unsaturated hydrocarbons [5–7]. We will highlight two GC-MC/MD studies; one assessing oxide formation in a Pd cluster as a function of oxygen pressure and temperature, and the other assessing carbide and hydride formation under varying hydrogen/hydrocarbon ratios in the gas phase. Together, these studies demonstrate the capabilities of the ReaxFF potential and the GC-MC/MD method for modeling *in situ* behavior in catalytic systems.

2. Theory and methods

2.1. ReaxFF potential

The ReaxFF potential [13] is a reactive force field comprised of bond-order/bond-length relationships [18,19] combined with polarizable charge descriptions [20] to describe covalent, Coulomb, and van der Waals interactions between atoms in a system. The bond-length/bond-order formalism yields a differentiable potential energy surface through reactive events, thus allowing for reactive molecular dynamics (RMD). As illustrated in Fig. 1, the transferability of the ReaxFF potential offers a unique capability for modeling catalyst behavior as a function of reaction conditions, since the same set of parameters can be employed in both GC-MC/MD simulations assessing *in situ* stability and in RMD simulations assessing kinetics.

The ReaxFF parameters unique to Pd/O and Pd/H interactions used herein were derived previously in [21] and in [22], respectively. We refer the reader to these publications and the references therein for detailed discussions of the accuracy of the ReaxFF method and the

* Corresponding authors.
E-mail addresses: acv13@psu.edu (A.C.T. van Duin), mjanik@psu.edu (M.J. Janik).

1566-7367/$ – see front matter © 2013 Elsevier B.V. All rights reserved.
http://dx.doi.org/10.1016/j.catcom.2013.12.001

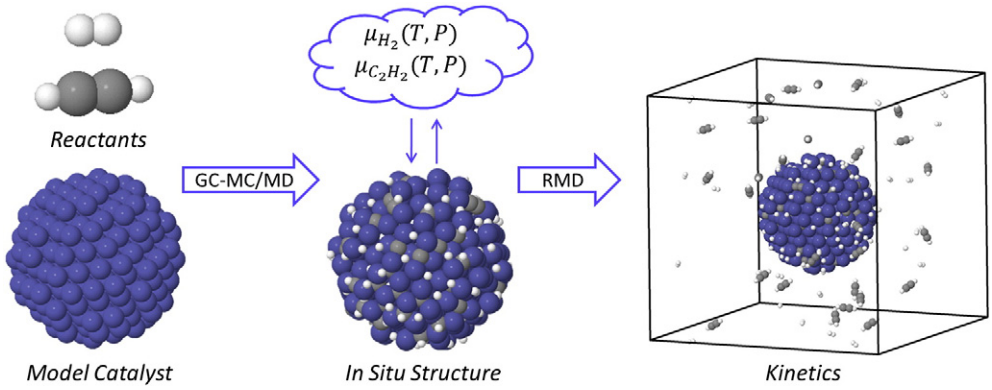

Fig. 1. Scheme for using GC-MC/MD and RMD in tandem.

parameter optimization process. The Pd/C/H potential parameters were similarly derived from a training set of ~40 data points consisting of C_xH_y adsorption energies at various surface, subsurface, and bulk Pd sites. Generally, the Pd/C/H ReaxFF parameters reproduce the adsorption energies in the training set to within an average of ~5 kcal mol^{-1}. ReaxFF and DFT adsorption energies on the energetically favored Pd(111) surface are briefly summarized in the supplemental material. The detailed contents of this training set and the parameter optimization process are beyond the scope of this communication, and will be fully described in forthcoming publications.

2.2. Grand canonical Monte Carlo

The recently developed [21] hybrid grand canonical-Monte Carlo/molecular dynamics (GC-MC/MD) method is well suited for investigating phase behavior, as it can model uptake of gas phase species in a solid. Atoms are stochastically exchanged between the system and a gas phase reservoir at constant chemical potential, $\mu_{res}(T, P)$, until the system reaches equilibrium with the gas phase reservoir. Here, the GC-MC/MD method is employed in a ($TVN_{Pd}\mu_{res}$) ensemble with constant temperature (T), volume (V), chemical potential of all species in the reservoir (μ_{res}) and number of Pd atoms (N_{Pd}). MC moves include insertion, deletion, or displacement of an atom other than Pd. The acceptance criteria for each move type is derived from detail-balance Boltzmann relationships [23], and are related to the temperature and pressure of the gas phase through the chemical potential of the reservoir, $\mu_{res}(T, P)$. Additionally, the GC-MC/MD method includes a MD-based energy minimization step after each MC move prior to applying the acceptance criteria. The bias toward acceptance introduced by the MD relaxation step is mitigated by excluding the volume occupied by Pd metal atoms from the total system volume definition utilized in the Boltzmann acceptance criteria, as described in [21]. This additional step allows for structural relaxation of the metal lattice necessary for forming new phases. Thus, the structure after GC-MC/MD reflects the stable phase in equilibrium with the gas phase at the temperature and pressure set by $\mu_{res}(T, P)$.

3. Results and discussion

Here we highlight two GC-MC/MD studies used to explore phase formation in Pd nanoparticles. The first assesses oxidation in a 3 nm Pd cluster as a function of oxygen pressure and temperature. The second demonstrates multi-species GC-MC/MD, in which both carbon and hydrogen atoms are exchanged with a hydrogen/hydrocarbon reservoir, showing the dependence of carbide/hydride formation on the ratio of reactant partial pressures in the gas phase.

3.1. Oxide formation in Pd

Oxide formation on palladium surfaces impacts the activity and selectivity of Pd-based catalysts, which are widely employed under oxygen rich operating conditions. Our recent study [21] applied the hybrid GC-MC/MD method to determine the extent of surface and bulk oxidation in Pd clusters. Oxygen atoms were added, moved, and removed from a 3 nm Pd cluster until the O:Pd ratio and total energy of the system converged. This method was repeated at varying temperatures and pressures to derive a theoretical phase diagram for the oxidation of Pd clusters in temperatures ranging from 300 K to 1300 K and oxygen pressures ranging from 10^{-14} atm to 1 atm, which is summarized in Fig. 2.

Fig. 2(a) reflects the convergence of O:Pd ratios in GC-MC/MD simulations at $P_{O2} = 1$ atm that correspond to three oxidation phases in the Pd cluster: (1) a bulk oxide at 500 K, (2) a surface oxide at 1000 K, and (3) Pd metal (no oxidation) at 1500 K. Intuitively, the phase transition between surface and bulk oxidation is marked by an increased O:Pd ratio. Additionally, the radial distribution of oxygen atoms in the cluster was analyzed to assess the extent of oxidation in surface and bulk regions of the cluster, which is demonstrated in Fig. 2(b). The radial distribution was calculated from the atomic coordinates of the final structure of the GC-MC/MD simulation, and represents the average number of oxygen atoms located at a specified radius, r, from the center of the cluster ($r = 0$). The radial distribution of oxygen atoms was determined for varying temperatures and oxygen pressures, allowing the thermodynamically stable phase to be determined for the specified oxygen pressure and temperature. Together, these data can be used to estimate oxidation phase boundaries, which are shown in the phase diagram in Fig. 2(c). In Fig. 2(c), each data point corresponds to a separate GC-MC/MD simulation for which the final structure was classified as either (1) a bulk oxide, (2) a surface oxide, or (3) Pd metal. The phase boundaries predicted by the ReaxFF GC-MC/MD method for the 3 nm cluster are similar to the experimental and *ab initio* phase boundaries reported by Ketteler et al. in [24] and by Lundgren et al. in [25] for single crystal Pd surfaces, as well as the experimentally observed bulk Pd → PdO phase boundaries reported by Zhang et al. in [26]. The ability to predict oxidation phase boundaries is instrumental to catalysis studies, as the degree of surface oxidation affects catalytic activity; which is experimentally demonstrated for methane combustion by Su et al. in [27] and for CO oxidation by Toyoshima et al. in [28].

3.2. Carbide and hydride formation in Pd

The GC-MC/MD method can also model the formation of multi-species phases that occur when the gas phase is composed of varying reactant compositions. Numerous studies suggest that the formation

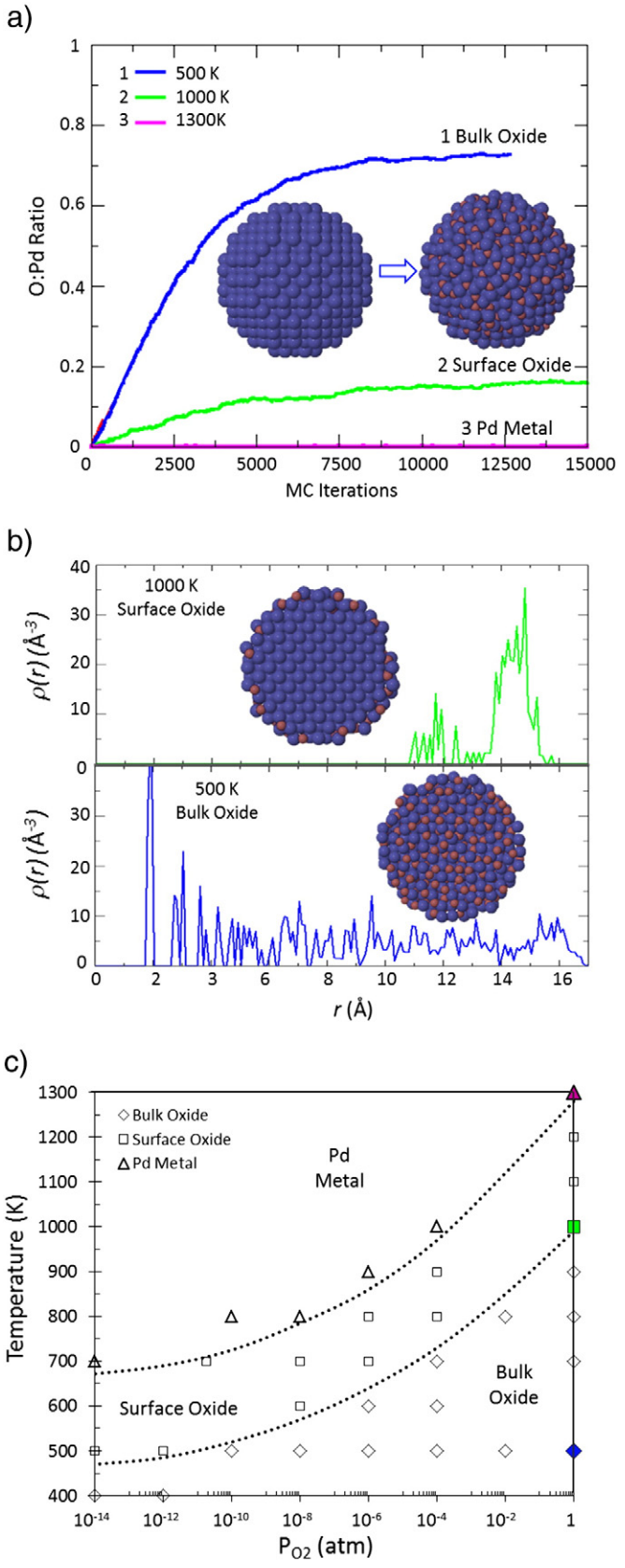

Fig. 2. (a) GC-MC/MD results for oxide formation in a 3 nm Pd cluster at $P_{O2} = 1$ atm. (b) Radial oxygen distribution, insets show center cross sections. (c) Oxidation phase diagram, data points represent separate GC-MC/MD simulations. The dotted boundaries represent estimated delineations between the oxidation phases, and the filled data points correspond to the simulations in (a) and (b). (Data adapted from Ref. [21]).

of a subsurface carbide phase enhances the selectivity of Pd catalysts toward hydrogenation. Teschner et al., using *in situ* X-ray photoelectron spectroscopy, found that a subsurface carbide phase is stable at low H:C ratios, yielding selective hydrogenation of 1-pentyne [5–7]. Total, unselective hydrogenation occurs at high H:C ratios after the subsurface carbide decomposes. They propose that the carbide phase separates bulk and surface hydrogen phases, thus inhibiting the more reactive bulk hydrogen from hydrogenating the hydrocarbon species on the surface of the cluster. We conducted GC-MC/MD simulations in which both C and H atoms were exchanged between a 2 nm Pd cluster and a hydrogen/hydrocarbon reservoir at 300 K, where μ_H and μ_C were determined by temperature and partial pressures in the reservoir. Each simulation was terminated after 6500 MC iterations, at which point the MC acceptance rates significantly decreased as the system approached equilibrium.

Fig. 3 summarizes the GC-MC/MD results for varying hydrogen and carbon pressures. Fig. 3(a–b) shows H/C:Pd ratios in simulations at the same hydrogen chemical potential and varying carbon chemical potentials, and *vice versa* in Fig. 3(c–d). As seen in Fig. 3(a–b), an increase in μ_C leads to an increase in both carbon *and* hydrogen uptake. Thus, an increase in the hydrocarbon pressure leads to increased hydrogen uptake, which corroborates the experimental finding of Teschner et al., who found that the H:Pd ratio increased from 0.75 after exposure to 1 atm of pure H_2 to 0.87 after hydrogenation events upon subsequent exposure to 1-pentyne [5]. Interestingly, Fig. 3(c–d) shows that the amount of carbon uptake is minimally affected by an increase in the hydrogen pressure. This can be explained by the radial distribution plots shown in Figs. 4 and 5. Results for low hydrogen pressure (10^{-14} atm) in Fig. 4 demonstrate that carbon preferentially aggregates in the subsurface region of the particle, and only begins to form surface hydrocarbon species at high hydrocarbon pressures. Fig. 5 summarizes carbon uptake at the same μ_C values, but at high hydrogen pressures (1 atm). In this case, the carbon still prefers the subsurface region, but forms surface hydrocarbons more readily.

The amount of carbon uptake in the particle is similar at both high and low hydrogen pressures, but the subsurface carbon phase is destroyed by the formation of surface hydrocarbon species at high hydrogen pressures. GC-MC/MD demonstrates that the subsurface carbon phase segregates surface and bulk hydrogen at low H:C ratios and that the extent of this segregation decreases at higher H:Pd ratios, in agreement with experimental observations [5–7].

4. Conclusion

We demonstrated the use of GC-MC/MD *via* the ReaxFF potential for modeling the structure and stability of phases that form in a Pd catalyst under reaction conditions typical of either oxidation or hydrogenation applications. The agreement between ReaxFF, *ab initio*, and experimental observations demonstrates the capability of the GC-MC/MD method for exploring the phase space of a catalyst under reaction conditions. Furthermore, the resultant system structures determined by GC-MC/MD can be utilized in subsequent RMD studies to assess reaction kinetics, or can be used to suggest models that better represent the catalyst surface under reaction conditions for more detailed DFT studies. The formalism presented here, though specifically tailored to Pd systems, can be readily extended to other catalytic systems, providing a new tool for exploring the impact of reaction conditions on catalyst activity, selectivity, and stability.

Acknowledgments

This research was supported by the National Science Foundation grant CBET-1032979.

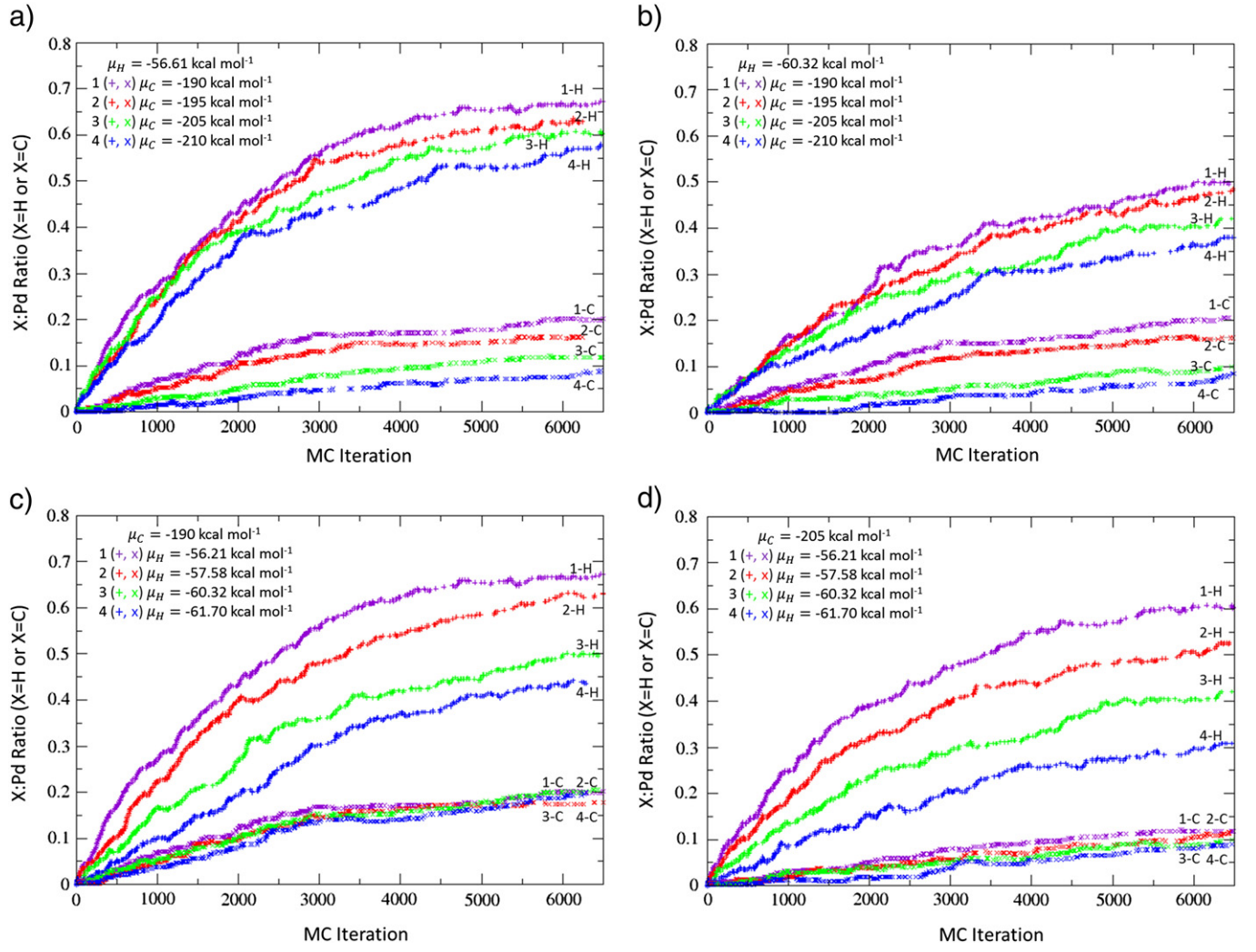

Fig. 3. GC-MC/MD results for hydrogen and carbon uptake in a 2 nm Pd cluster at 300 K and at constant (a–b) hydrogen chemical potential, or (c–d) carbon chemical potential. "+" symbols represent hydrogen data and "×" symbols represent carbon data. A less negative hydrogen chemical potential indicates a higher effective H_2 pressure.

Appendix A. Supplementary data

Supplementary data to this article can be found online at http://dx.doi.org/10.1016/j.catcom.2013.12.001.

References

[1] K. Tanaka, Catal. Today 154 (2010) 105–112.
[2] L.P. Nielsen, F. Besenbacher, E. Laegsgaard, I. Stensgaard, Phys. Rev. B 44 (1991) 13156–13159.
[3] A. Hellman, A. Resta, N.M. Martin, J. Gustafson, A. Trinchero, P.A. Carlsson, O. Balmes, R. Felici, R. van Rijn, J.W.M. Frenken, J.N. Andersen, E. Lundgren, H. Grönbeck, J. Phys. Chem. Lett. 3 (2012) 678–682.
[4] J. Klikovits, M. Schmid, L.R. Merte, P. Varga, R. Westerström, A. Resta, J.N. Andersen, J. Gustafson, A. Mikkelsen, E. Lundgren, F. Mittendorfer, G. Kresse, Phys. Rev. Lett. 101 (2008) 266104.
[5] D. Teschner, J. Borsodi, A. Wootsch, Z. Révay, M. Hävecker, A. Knop-Gericke, S.D. Jackson, R. Schlögl, Science 320 (2008) 86–89.
[6] D. Teschner, J. Borsodi, Z. Kis, L. Szentmiklósi, Z. Révay, A. Knop-Gericke, R. Schlögl, D. Torres, P. Sautet, J. Phys. Chem. C 114 (2010) 2293–2299.
[7] E.M. Vass, M. Hävecker, S. Zafeiratos, D. Teschner, A. Knop-Gericke, R. Schlögl, J. Phys. Condens. Matter 20 (2008) 184016.
[8] K. Reuter, M. Scheffler, Phys. Rev. B 65 (2001) 035406.
[9] K. Reuter, M. Scheffler, Phys. Rev. Lett. 90 (2003) 046103.
[10] C.l. Chizallet, G.t. Bonnard, E. Krebs, L. Bisson, C.c. Thomazeau, P. Raybaud, J. Phys. Chem. C 115 (2011) 12135–12149.
[11] N. İnoğlu, J.R. Kitchin, J. Catal. 261 (2009) 188–194.
[12] A.D. Mayernick, M.J. Janik, J. Chem. Phys. 131 (2009) 084701–084712.
[13] A.C.T. van Duin, S. Dasgupta, F. Lorant, W.A. Goddard III, J. Phys. Chem. A 105 (2001) 9396–9409.
[14] G.B. Hoflund, H.A.E. Hagelin, J.F. Weaver, G.N. Salaita, Appl. Surf. Sci. 205 (2003) 102–112.
[15] R.V. Gulyaev, A.I. Stadnichenko, E.M. Slavinskaya, A.S. Ivanova, S.V. Koscheev, A.I. Boronin, Appl. Catal. A Gen. 439–440 (2012) 41–50.
[16] T. Engel, G. Ertl, J. Chem. Phys. 69 (1978) 1267–1281.
[17] J.Y. Han, D.Y. Zemlyanov, F.H. Ribeiro, Surf. Sci. 600 (2006) 2730–2744.
[18] D.W. Brenner, Phys. Rev. B 42 (1990) 9458–9471.
[19] J. Tersoff, Phys. Rev. Lett. 61 (1988) 2879–2882.
[20] W.J. Mortier, S.K. Ghosh, S. Shankar, J. Am. Chem. Soc. 108 (1986) 4315–4320.
[21] T.P. Senftle, R.J. Meyer, M.J. Janik, A.C.T. van Duin, J. Chem. Phys. 139 (2013) 044109–044115.
[22] T.P. Senftle, M.J. Janik, A.C.T. van Duin, J. Phys. Chem. C (2013)(submitted for publication).
[23] D. Frenkel, B. Smit, Understanding Molecular Simulation, Academic Press, San Diego, 2002.
[24] G. Ketteler, D.F. Ogletree, H. Bluhm, H.J. Liu, E.L.D. Hebenstreit, M. Salmeron, J. Am. Chem. Soc. 127 (2005) 18269–18273.
[25] E. Lundgren, J. Gustafson, A. Mikkelsen, J.N. Andersen, A. Stierle, H. Dosch, M. Todorova, J. Rogal, K. Reuter, M. Scheffler, Phys. Rev. Lett. 92 (2004) 046101.
[26] H. Zhang, J. Gromek, G. Fernando, H. Marcus, S. Boorse, J. Phase Equilib. Diffus. 23 (2002) 246–248.
[27] S.C. Su, J.N. Carstens, A.T. Bell, J. Catal. 176 (1998) 125–135.
[28] R. Toyoshima, M. Yoshida, Y. Monya, K. Suzuki, B.S. Mun, K. Amemiya, K. Mase, H. Kondoh, J. Phys. Chem. Lett. 3 (2012) 3182–3187.

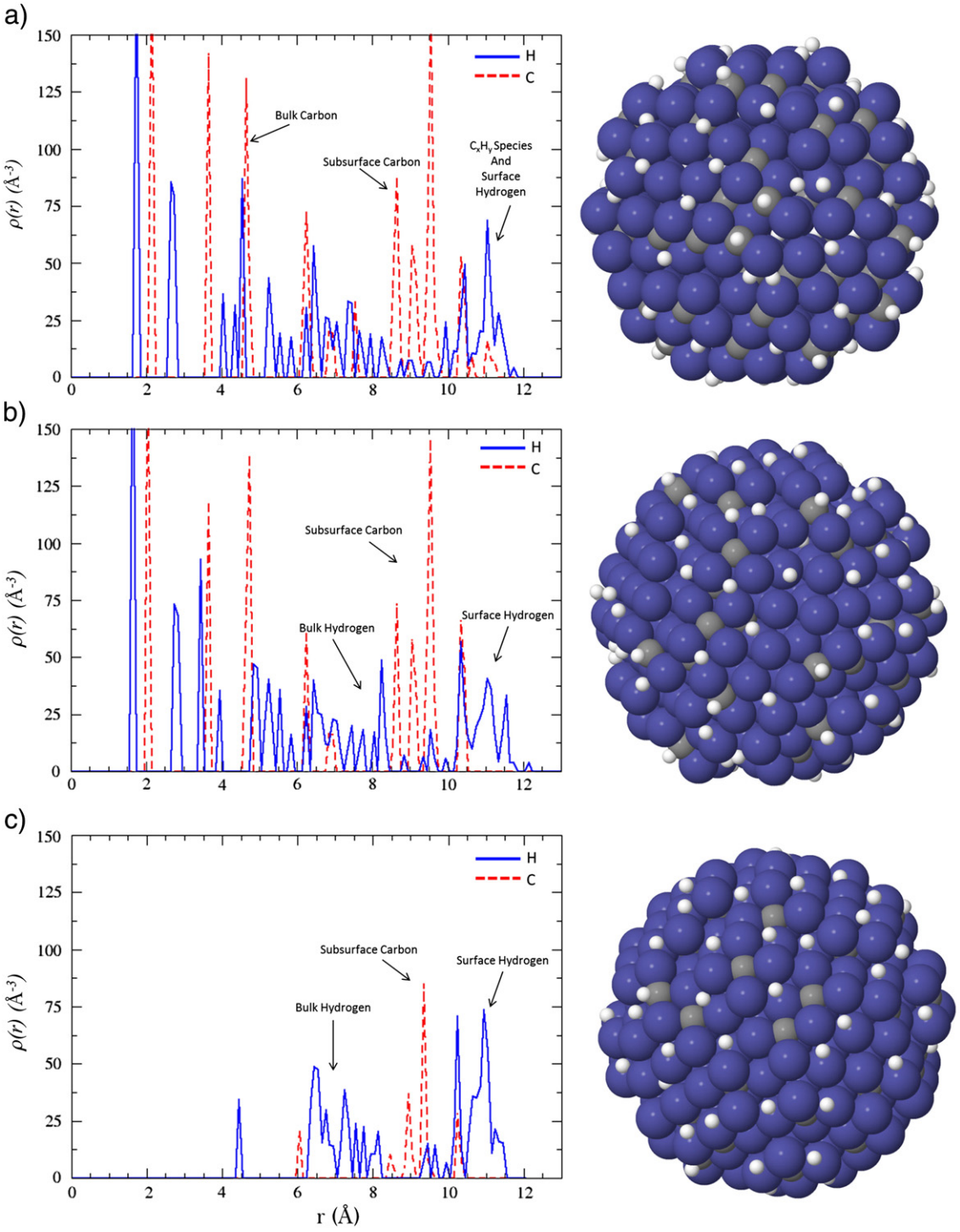

Fig. 4. Radial distribution of carbon and hydrogen after GC-MC/MD at 300 K, $\mu_H = -65.82$ kcal mol^{-1} ($P_{H2} = 10^{-14}$ atm) and (a) $\mu_C = -190.0$ kcal mol^{-1}, (b) $\mu_C = -195.0$ kcal mol^{-1}, or (c) μ_C–200.0 kcal mol^{-1}.

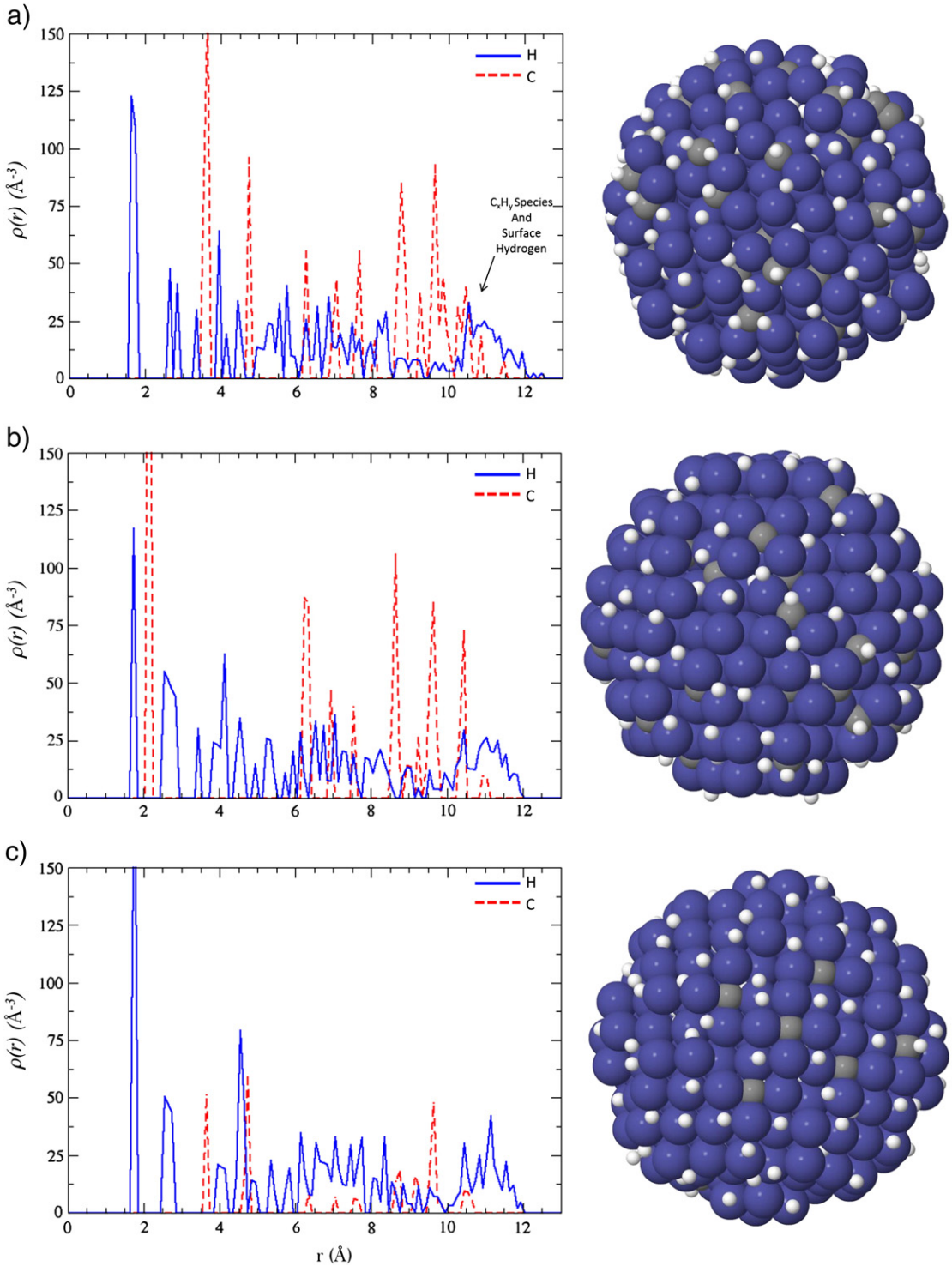

Fig. 5. Radial distribution of carbon and hydrogen after GC-MC/MD at 300 K, $\mu_H = -56.21$ kcal mol^{-1} ($P_{H2} = 1$ atm) and (a) $\mu_C = -190.0$ kcal mol^{-1}, (b) $\mu_C = -195.0$ kcal mol^{-1}, or (c) μ_C–200.0 kcal mol^{-1}.